

Characterization and Optimization of Persian Gum/Whey Protein Bionanocomposite Films Containing Betanin Nanoliposomes for Food Packaging Utilization

Zahra Ghasempour

Tabriz University of Medical Sciences

Sepideh Khodaivandi

Department of Higher Education

Hossein Ahangari

Tabriz University of Medical Sciences

Hamed Hamishehkar

Tabriz University of Medical Sciences

Sajed Amjadi

Urmia University

Ehsan Moghaddas Kia (✉ ehsan.m.kia@gmail.com)

Maragheh University of Medical Sciences <https://orcid.org/0000-0002-1032-7264>

Ali Ehsani

Tabriz University of Medical Sciences

Research Article

Keywords: Biopolymers, Biodegradable materials, Packaging film, Functional properties, Nanoliposomes

Posted Date: April 27th, 2021

DOI: <https://doi.org/10.21203/rs.3.rs-420388/v1>

License:  This work is licensed under a Creative Commons Attribution 4.0 International License.

[Read Full License](#)

Version of Record: A version of this preprint was published at Journal of Polymers and the Environment on January 31st, 2022. See the published version at <https://doi.org/10.1007/s10924-021-02367-0>.

Characterization and Optimization of Persian Gum/Whey Protein Bionanocomposite Films Containing Betanin Nanoliposomes for Food Packaging Utilization

Running title: Biocomposite edible film containing betanin nanoliposomes

Zahra Ghasempour ^{a,b}, Sepideh Khodaeivandi ^c, Hossein Ahangari ^a, Hamed Hamishehkar ^b, Sajed Amjadi ^d, Ehsan Moghaddas Kia ^{e*}, Ali Ehsani ^{a,b*}

^a Department of Food Science and Technology, Faculty of Nutrition and Food Sciences, Tabriz University of Medical Sciences, Tabriz, Iran

^b Drug Applied Research Center, Tabriz University of Medical Sciences, Tabriz, Iran

^c Department of Food Science and Technology, Afagh Higher Education Institute, Urmia, Iran

^d Department of Food Science and Technology, Urmia University, Urmia, Iran

^e Department of Food Science and Nutrition, Maragheh University of Medical Sciences, Maragheh, Iran

***Correspondence;** Ehsan Moghaddas Kia- Ali Ehsani

E.mail: ehsan.m.kia@gmail.com , ehsani@tbzmed.ac.ir ,

Tel: +989144403254, +989144395097

1 **Abstract**

2 In this study, composite packaging films were produced from relatively inexpensive materials
3 including whey protein isolate (WPI) and Persian gum (PG), supplemented with betanin
4 nanoliposomes (NLPs). Using response surface methodology (central composite design), we
5 investigated the effects of two variables (PG [0-2% w/v] and betanin NLPs' [0-10% w/v]
6 content) on the physico-mechanical and antioxidant properties of the film treatments.
7 Afterward, the optimal treatment was evaluated for structural and antimicrobial characteristics.
8 The film samples' permeability to water vapor decreased with the addition of NLP (from 7.38
9 to 5.46 g/Pa.s.m) but increased with PG incorporation; decreased solubility was observed when
10 either substance was added. Mechanical properties like Young's modulus and tensile strength
11 were weakened by PG addition, but the incorporation of NLPs led to pronounced tensile
12 strength. XRD analysis revealed improved crystallinity through NLPs' addition. The presence
13 of NLPs in the nanocomposite film resulted in an elevated level of antibacterial activity against
14 *Staphylococcus aureus*, while the addition of both PG and betanin NLPs led to improved
15 antioxidative activity (63.45%). Considering the results, PG/WPI films loaded with betanin
16 NLPs could be introduced in active packaging applications for the shelf life extension of
17 perishable food products.

18 **Keywords:** Biopolymers; Biodegradable materials; Packaging film; Functional properties;
19 Nanoliposomes

20 **1. Introduction**

21 Environmental pollution represents an inevitable consequence of the utilization of non-
22 biodegradable plastic materials in food packaging systems. However, growing demands among
23 consumers for safe, high-quality foods have led to pronounced scientific interest in the
24 enhancement of bio-based polymer packaging materials [1]. Biopolymer films are preferred
25 because of their edibility, biocompatibility, rapid biodegradation, and the potential to act as
26 vehicles for bioactive substances; drawbacks like water susceptibility and poor mechanical
27 characteristics must also be noted [2]. Owing to such drawbacks, the industrial-scale
28 fabrication of natural, polymer-based packaging films has been limited [3].

29 Most protein-based edible films act as impressive gas barriers while possessing more desirable
30 mechanical properties relative to films based on fats and polysaccharides. Whey proteins are
31 byproducts of the cheese-making process, purified via ultrafiltration and diafiltration. Whey-
32 based edible films are appreciated for their stable mechanical characteristics and demonstrate
33 good gas barrier resistance while acting as noticeable barriers to edible oils and aromatic
34 compounds. Nevertheless, films based on hydrophilic proteins like whey show a moderate level
35 of moisture resistance [4]. Several methods exist to develop the properties of edible protein
36 films, including physical techniques, enzymatic methods, and strategies involving their
37 combination with hydrophobic substances such as gums.

38 Persian gum (PG), also named Zedo and Angum, is a natural and low-cost biopolymer that is
39 extracted from *Amygdalus scoparia* Spach (the mountain almond tree), which grows naturally
40 in Iran's forests. Considering its dry weight, PG is constituted by polysaccharides (mainly
41 galactopyranosyl and arabinofuranosyl polysaccharides) and a scarce amount of proteins,
42 thereby having a high water absorption capacity [5, 6]. The adverse ratio of Ara:Gal, the low
43 protein content and the existence of xylose and mannose were highlighted as a distinguishing
44 feature compared to gum Arabic. PG contains 82–90% w/w carbohydrate, around 0.19% w/w

45 lipid, 0.20–1.02% w/w protein, and 0.60% w/w tannins. The ash content (1.66–3.63% w/w)
46 and the elements (Na, K, Zn, Fe, Mg, Ca) vary widely. Abbasi [7] described the medicinal and
47 health-promoting actions of PG, including mucus reduction, healing of swollen joints, and
48 acting as a remedy for tooth pain. This anionic hydrocolloid possesses emulsifying properties
49 that are similar to those of gum Arabic; it forms brittle films that can be developed by applying
50 a plasticizer [8]. Recently, several investigations have elucidated the capacity of PG in the
51 preparation of edible films or coatings [8-12]. Likewise, the interaction of PG with whey
52 proteins and β -lactoglobulin has been investigated, where the potentiality of these interactions
53 for film-forming solutions was remarked [13, 14].

54 Packaging fulfills a critical role in food preservation, and the incorporation of
55 antimicrobial/antioxidant agents into film materials is a suitable approach to promote active
56 packaging. It is reported that the addition of these bioactive substances to packaging materials
57 confers more benefits than their direct application to food surfaces.

58 Betalains are water-soluble and nitrogen-containing pigments found in high concentrations in
59 red beet and they comprise two sub-classes: betaxanthins and betacyanins. As the predominant
60 type of betacyanins, betanin (betanidin 5-O-D-glucoside [schematic 1]; code: E 162) is known
61 as an approved colorant in cosmetic, pharmaceutical, and food products. Betanin is approved
62 as a Generally Recognized as Safe (GRAS) food additive, which can be added to foods as an
63 antioxidant and colorant agents [15, 16]. Some biological functions such as the inhibition of
64 lipid oxidation and the provision of cardioprotective, hepatoprotective, anti-inflammatory, anti-
65 proliferative, and antimicrobial effects are mentioned for this bioactive pigment. Betanin is an
66 unstable substance, and its stability during storage can be affected by factors such as exposure
67 to light, extreme pH, enzymes, high temperature, and oxygen. During the process of betanin
68 decomposition, cyclo-dopa-5-O-glycoside and betalamic acid are formed; these products lack
69 the bioactivity of pure betanin [17, 18].

70 Bio-nanocomposites are a new generation of biodegradable packagings made from the
71 combination of inorganic/organic materials and biopolymers with the presence of at least one
72 active nano-based compound. Among the advantages of producing bio-nanocomposites is the
73 application of materials that improve the production efficiency, barrier properties, UV-
74 shielding ability, and overall physico-chemical characteristics of the final product [9].

75 Lipid-based nano-carriers, among them nanoliposomes are desired, because of capability to
76 encapsulate both hydrophobic and hydrophilic ingredients and their amphiphilicity,
77 biocompatibility, non-immunogenicity, and non-toxicity considering the endogenic nature of
78 their constituents. In this study, given our positive experience with the use of liposomes as wall
79 materials for betanin stabilization [19, 20], we aimed to develop PG/whey protein-based
80 biocomposite films embedded with betanin nanoliposomes (NLPs). Furthermore, we
81 characterized the effects of betanin NLPs and PG on the water vapor permeability, thickness,
82 antioxidant activity, mechanical properties, color parameters, morphology, and antimicrobial
83 activity of the fabricated bio-nanocomposites.

84

85 **2. Experimental**

86 **2.1. Materials**

87 Whey protein isolate (WPI; protein 921.6 g/kg as determined by manufacturer) was procured
88 from German Prot, Sachsenmilch Lepperrsdorf GmbH (Saxony, Germany). Dried PG granules
89 were obtained from a reputable herbal market (Shiraz, Iran). The gum kernels were categorized
90 into red, yellow, and white according to their quality and color. Then, the qualified white and
91 yellow gum samples were powdered by a mechanical blender and sieved carefully to obtain a
92 uniform particle size of less than 500 μm ; the average molecular weights were 8.4×10^2 and
93 4.7×10^3 kDa, respectively. Lecithin was purchased from Lipoid Co. (Ludwigshafen, Germany).
94 Betanin, glycerol, 2,2-diphenyl-1-picrylhydrazyl (DPPH), and other analytical grade solvents

95 and reagents were procured from Sigma-Aldrich (St. Louis, USA); deionized water was used
96 during the experiments.

97 **2.3. Preparation of biocomposite films**

98 Betanin NLPs were prepared by employing the thin film hydration-sonication method
99 described in our previous study [20]. Edible films containing different ratios of PG and NLPs
100 were prepared according to the experimental design. Biocomposite films were made by gently
101 dissolving PG (0–2 %) in distilled water for 1 h at 90 °C. PG dispersions were hydrated
102 overnight at room temperature before WPI was applied in a ratio of 5% w/v and the mixture
103 was mixed for 30 min at 80 °C. In this way, the ratios of WPI to PG were set in the ranges from
104 5:0 to 5:2. Subsequently, the NLPs were added at levels of 0-10%, and the mixture was
105 subjected to 15 min of vigorous shaking at 40 °C. Then, glycerol was added at a constant
106 volume of 40% w/v of dry matter (WPI) for all samples. The pH of the solutions was set at 9
107 using NaOH before 20 mL dispersions were cast into glass plates. Ultimately, the films were
108 peeled off and re-conditioned at $53 \pm 1\%$ relative humidity (RH) and 25 °C for 48 h.

109 **2.4. Characterization of films**

110 **2.4.1. Water vapor permeability (WVP)**

111 In line with the procedure described by Khezerlou, Ehsani [9], the WVP of the samples was
112 obtained gravimetrically. Firstly, constant amounts of anhydrous CaCl_2 were weighed in cells
113 and then sealed with film samples using liquified paraffin. Next, the RH within the desiccators
114 was adjusted to 75% using saturated NaCl solution, and alterations in the cell weights were
115 recorded every 6 h till reaching a stable weight. Also, the system's weight gain was measured
116 to determine water transfer over the film samples. Ultimately, the mass changes of the
117 permeation cells were plotted against time; the slope of the function was fitted with linear
118 regression ($R^2 > 0.999$), and the water vapor transmission rate (WVTR) was estimated according
119 to the following equation:

120 $WVTR = \text{slope}/(\text{exposed film area}): \Delta m/\Delta t \times \frac{1}{A}$ (1)

121 It should be noted that the thickness of the film samples was measured beforehand. Finally, the
122 WVP ($gPa^{-1}s^{-1}m^{-1}$) was calculated using Equation 2:

123 $WVP = \Delta m/(\Delta t \times A) \times \frac{x}{\Delta p}$ (2)

124 where $\Delta m/\Delta t$ represents the moisture uptake over time (g/s), X is the thickness average (mm),
125 A is the area of the exposed film samples (m^2), and Δp is the difference of water vapor pressure
126 between inside and outside of the cell.

127 **2.4.2. Film solubility in water**

128 The film samples were kept overnight in a desiccator in the presence of calcium sulfate, before
129 the films ($W_i \sim 400$ mg) were mixed with a constant amount of distilled water for 24 h at room
130 temperature. Finally, the remained samples were transferred to the oven $105^\circ C$ [21]. The dried
131 films were then weighed to obtain the final weight (W_f), and water solubility was calculated
132 according to Equation 3:

133 $Water\ solubility\ (\%) = \frac{W_i - W_f}{W_i} \times 100$ (3)

134 **2.4.3. Determination of antioxidant activity**

135 For the assessment of antioxidant activity, 25 mg of films were submerged in 4 mL of distilled
136 water under constant stirring; then, 2 mL of the solution was incubated with 2 mL of 0.1 mM
137 DPPH methanolic solution. The resultant mixture was kept in dark at room temperature for one
138 hour. Subsequently, the sample absorbance was measured at 517 nm using a UV-Vis
139 spectrophotometer (Model T60 UV, USA). The free radical scavenging activity was
140 approximated using Equation 4:

141 $DPPH\ scavenging\ activity\ (\%) = \frac{Abs_c - Abs_s}{Abs_c} \times 100$ (4)

142 where Abs_c is the absorbance of the blank DPPH and Abs_s is the absorbance of the samples
143 [22].

144 **2.4.4. Mechanical properties**

145 For each film sample, the ultimate tensile strength (UTS) and Young's modulus (YM) were
146 evaluated at room temperature with a universal testing machine (Model H100K-S, England)
147 according to the standard ASTM E96 method. To this end, the test samples were each cut into
148 a specific shape featuring width and length of 10 and 80 mm, respectively. The gauge size and
149 crosshead speed were 50 mm and 10 mm/min, respectively. Three replicates were done for
150 each process [23].

151 **2.4.5. Instrumental color analysis**

152 The primary color factors were evaluated using a colorimeter (Color Flex, M/s Hunter
153 Colorlab, USA). The parameters measured included L* and a*. The film samples were
154 positioned on a standard white plate.

155 **2.4.6. Scanning electron microscopy (SEM)**

156 The morphological properties of the films' surface and fracture structure were examined with
157 an SEM apparatus (Hitachi 4300S, Japan) at room temperature. The used voltage was 5.0 kV,
158 and the surface was coated by gold with a thickness of a few nanometers. For cross-sectional
159 analysis, the samples were visualized perpendicular to the fracture surface.

160 **2.4.7. X-ray diffraction (XRD) analysis**

161 The films' XRD measurement was completed using a Bruker D8 ADVANCE X-ray
162 diffractometer (Karlsruhe, Germany) working at a Cu K α wavelength of 0.154 nm. The
163 samples were contacted to the X-ray beam with the generator operating at 40 kV and 40 mA.
164 The distributed radiation was identified at room temperature over the range of diffraction angle
165 $2\theta = 2^\circ - 40^\circ$ at a rate of $1^\circ/\text{min}$ with a step size of 0.02° [24].

166 **2.4.8. Antimicrobial activity**

167 The inhibition zone method was implemented for the examination of the films' antimicrobial
168 assay against *Staphylococcus aureus* (ATCC 43300) and *Escherichia coli* O157: H7 (ATCC

169 35218) as typical Gram-positive and Gram-negative pathogenic microorganisms, respectively.
170 To this end, 10 mL of molten Brain Heart Infusion (BHI) agar was poured into plates to which
171 200 μ L of the bacterial cultures, featuring colony counts of 10^8 CFU/mL, were added. The film
172 discs were prepared and situated on the bacterial lawn which were incubated at 37 °C for 24 h
173 in an incubator. On the following day, the plates were evaluated for the inhibition zone of the
174 film discs. The diameter of the whole zone was determined and then subtracted from the film
175 disc's diameter.

176 **2.5. Statistical design, analysis, and optimization**

177 In this study, we applied central composite design with two independent variables, namely the
178 levels of betanin NLPs (0-10% w/v) and PG (0-2% w/v), with no blocking of the experiments,
179 resulting in 13 film treatments. Betanin NLPs and PG were considered as continuous numeric
180 variables. Statistically, p-values of less than 0.05 were regarded as significant. Second-order
181 polynomial modeling and data analysis were accomplished using Design Expert 10 (USA)
182 statistical software.

183 In the next step, the optimum point was obtained considering the following goals: maximizing
184 the antioxidant capacity, UTS, a^* (redness), and antimicrobial activity of the film, while
185 minimizing its WVP, water solubility, and lightness. The optimum treatment was investigated
186 for structural, morphological, and antimicrobial properties.

187 **3. Results and Discussion**

188 **3.1. Water vapor permeability (WVP)**

189 In packaging materials, low WVP values are desired for the extension of food shelf life as
190 highly permeable films facilitate rapid product spoilage. Another key parameter is the WVTR,
191 which reflects the hydrophilicity or hydrophobicity of the edible film, where hydrophilic films
192 have higher WVTR values. The contour plots of WVP as a function of NLP and PG
193 concentrations are shown in Figure 1. Our results indicated that the interaction effect of PG

194 and NLP addition on WVP was significant ($P < 0.05$). The WVP capacity of edible films
195 increased with higher PG concentrations but declined with the loading of NLPs to PG-
196 containing films. Polysaccharides promote water permeation despite their suitable barrier
197 properties against gases [11]. However, the incorporation of lecithin NLPs decreases the WVP,
198 water absorption capacity, and moisture content of film samples [25]. In fact, the addition of
199 NLPs to protein films can exert a plasticizing effect and decrease the film's solubility, thereby
200 lowering its WVP. The NLPs, which are located in the links between the polymer matrixes,
201 inhibit gas and water diffusion across the film [26]. Previously, similar trends were reported
202 by Zhang, Liu [27], who showed that WVP declined by about 189% with the loading of only
203 5% lignin NLPs into a polyvinyl alcohol nanocomposite. However, as reported by Cejudo-
204 Bastante, Cejudo-Bastante [28], red beet extract addition, without wall material, into film
205 material caused an increment in WVP.

206 **3.2. Water solubility**

207 According to the data analysis, the interaction effect of NLPs and PG on solubility was
208 significant ($P < 0.05$). Through the simultaneous incorporation of NLPs and PG, the film
209 solubility declined. The lowest solubility was obtained in the treatment with 10% NLPs and
210 2% PG. Solubility is related to both the hydrophilic/hydrophobic ratio of liposomes and the
211 number of free hydroxyl groups in the polymer matrix available for hydrogen bonding with the
212 polymers [29]. In the case of PG, the reduction in solubility can be attributed to the polymer
213 constituents (soluble and insoluble fraction) and the reaction between the anionic PG and the
214 positively charged protein in the film structure [5, 6]. Moreover, NLPs can bond with
215 macromolecules, restricting molecular movement and thereby reducing the film's water
216 solubility [30]. The notable point is that due to the significance of water solubility for the
217 transportation of bioactive substrates, WPI/PG-based films can be proper instruments for the
218 entrapment of bioactive compounds such as betanin and other anthocyanins. In line with our

219 observations, Alizadeh-Sani, Khezerlou [31] found that the incorporation of rosemary essential
220 oil into a WPI-based film resulted in a meaningful decrease in the film's water solubility (from
221 46.66 to 25.33%) and water content.

222 **3.3. Antioxidant activity**

223 As a stable synthetic radical, DPPH binds to hydrogen atoms in a process that can be monitored
224 through the amount of pure violet color loss or the decrease in absorbance. The obtained results
225 confirmed that both NLPs and PG significantly improved the film's antioxidant capacity
226 ($P < 0.05$); a high adjusted R^2 value (0.99) was attained for the related predictive model (Table
227 1). According to the contour plot shown in Figure 2, by increasing the amounts of both PG and
228 NLPs, the antioxidant capacity of the film improved from 30 to 75%. While such antioxidative
229 activity is due to the presence of both PG and NLPs, the latter provides the major effect. Betanin
230 (betanidin 5-O-D-glucoside) is recognized as a powerful antioxidant that exhibits excellent
231 radical-scavenging activity. Persian gum-based polymer structures contain numerous
232 arabinogalactans and probably possess antioxidative activity [32]. Our results are in agreement
233 with those of Amjadi, Nazari [20], who demonstrated that film samples containing uncoated
234 betanin or betanin NLPs offered greater antioxidant activity than control samples and that
235 encapsulation with NLPs protected the betanin and augmented its antioxidative activity from
236 6.79 to 53.02%.

237 **3.4. Mechanical properties**

238 Films that maintain high UTS are considered suitable for packaging applications. The effects
239 of NLPs and PG on the UTS of the samples were significant ($P < 0.05$) and are depicted in
240 Figure 3A. Notably, the maximum increment in UTS (from 1.95 to 4.96 Mpa) was achieved
241 by the addition of 5% NLPs and 1% PG. In a study by Pak, Ghaghelestani [8], it was reported
242 that the UTS of edible films containing PG was related to the gum/plasticizer ratio, such that
243 increased gum content caused a reduction in tensile strength. The increment in UTS with higher

244 betanin NLP concentrations may be ascribed to the existence of lecithin (as a component of the
245 NLPs) in the film's polymer structure. The incorporation of NLPs into protein films can exert
246 a plasticizing effect and improve film extensibility. The NLPs can expand the film's tensile
247 strength secondary to an intensified interaction between the NLPs and the protein matrix [26].
248 In this regard, Aziz and Almasi [24] found that by the addition of 15% *Thymus vulgaris* L.
249 extract NLPs to WPI films, the UTS increased from 2.09 to 8.67 Mpa, which is consistent with
250 our data.

251 Young's modulus (YM) or elasticity is a mechanical property that reflects the stiffness of a
252 packaging film, defined as the association between stress (force per area unit) and strain
253 (relational deformation) in the linear elasticity of a uniaxial deformation. Our results indicated
254 that in the films containing both PG and betanin NLPs, an increase in PG concentration caused
255 a significant decrement ($P < 0.05$) in YM from 84.12 to 42.43 MPa. Figure 3B demonstrates the
256 effect of betanin NLPs and PG on the YM of the film samples. These findings are in line with
257 the results of Ghadetaj, Almasi [33], who incorporated the NLPs of *Grammosciadium*
258 *ptrocarpum* Bioss. essential oil into WPI-based films and found that by the addition of 0 to
259 1.5% NLPs, the YM decreased significantly from 23.229 to 17.022 MPa ($P < 0.05$). These
260 researchers noted that this was because the essential oil molecules lowered the molecular
261 strength of the film by diminishing the intramolecular relations present within the protein
262 matrix. The remarkable effects of PG in the reduction of the UTS and YM of edible films
263 containing gelatin and tragacanth gum were also reported by Khodaei, Oltrogge [10].

264 **3.5. Color parameters**

265 Optical parameters such as color and transparency represent significant aspects pertaining to
266 consumer acceptance. The measured color parameters were L^* and a^* , which indicate the
267 amount of lightness and redness/greenness, respectively. The results implied a significant effect
268 of PG content on L^* ($P < 0.05$), while the effect of incorporating betanin NLPs was insignificant

269 (P>0.05). With the addition of 2% PG, the L* value decreased from 75 to 55. Pak,
270 Ghaghelestani [8] explained that changes in the L* parameter in the presence of PG may be
271 directly related to the homogeneity of the matrix, such that higher homogeneity results in
272 greater transparency.

273 The a* (red/green) index significantly increased with the incorporation of betanin NLPs but
274 decreased with PG addition. In this view and in agreement with our results, Amjadi, Nazari
275 [20] manufactured a nanocomposite film containing 10% betanin NLPs and found that the L*
276 value increased from 36.70 to 37.56 and the a* value increased from 15.52 to 18.24. It seems
277 obvious that the fall in a* with PG loading is due to the turbidity induced by the presence of
278 this gum in the film.

279 **3.6. Optimization**

280 The main objective of this study was to evaluate the effect of betanin NLP and PG incorporation
281 on the structural and functional features of an edible film. As presented in Table 1, the
282 polynomial second-order models were fitted to the data for each dependent variable through
283 multiple regression analyses. Regression analysis was applied to model different responses as
284 a function of the concentrations of betanin NLPs and PG. The regression coefficients are
285 closely related to the factor effects; the higher the coefficient the higher the effect of that term
286 in the model.

287 The response surface methodology (RSM) was used for the optimization, and the desirability
288 function for each response was assessed by numerical methods to obtain the overall
289 desirability. The responses of the optimal film are shown in Table 2. The optimal formulation
290 for the whey protein-based film was obtained with a betanin NLP content of 6.90% and a PG
291 concentration of 1.5%. Also, the overall utility of the predicted area for the available variables
292 was 0.718. For reproducibility, two optimal samples were produced, and then tests were

293 repeated three times to confirm the accuracy. The optimum treatment was investigated in terms
294 of its structural (SEM and XRD) and antimicrobial characteristics.

295 **3.6.1. Scanning electron microscopy (SEM)**

296 Scanning electron microscopy is a useful instrument for the evaluation of the surface and
297 morphological aspects of nanostructures. According to our results, the surface of the control
298 film was soft, continuous, and free of pores (Figure 4A). In contrast, the surface of the optimum
299 treatment had greater roughness (Figure 4B). It must be noted that WPI-based films maintain
300 a fully compact structure, with the spatial position of the polymers remaining consistent within
301 the matrix and thereby preventing surface roughness. This could be related to the hydrophilicity
302 of the proteins during phase separation. Corresponding with our results, Acquah, Zhang [34]
303 reported that WPI films were observed to be homocomposites that formed continuous
304 structures.

305 **3.6.2. X-ray diffraction (XRD) study**

306 The XRD spectra of the pure WPI, the PG, and the betanin NLPs are displayed in Figure 5
307 along with that of the optimal film sample. Crystal planes originate from crystal lattices and
308 are employed to determine the structure and shape of the unit cell and crystal lattice [20].
309 Images of XRD provide structural information, including that of crystalline and amorphous
310 polymeric structures like edible films. In XRD spectra, sharp diffraction peaks represent
311 crystalline diffraction. The XRD results elucidated a crystalline structure for pure WPI films;
312 the peak at $2\theta = 25^\circ$ indicates that the WPI crystallinity was relatively high. Therefore, the
313 application of the WPI component contributes to the semi-crystalline nature of the biopolymer.
314 Persian gum showed a vast peak at $2\theta = 25^\circ$, and the crystallographic index for WPI and PG
315 were 26.45 and 23.11%, respectively. The XRD results for the pure betanin sample featured a
316 broad peak at $2\theta = 22^\circ$. In the NLP-containing films, the mentioned peak intensity did not vary
317 considerably from that of the control sample. This implies that the amphiphilic lecithin

318 molecules in the NLPs interacted with the matrix proteins. Hence, the addition of NLPs not
319 only had no adverse effects on the film structure but also increased the film's density, thereby
320 protecting its crystalline nature. These results indicated a high level of affinity between the
321 WPI and the added betanin NLPs. The observed phenomenon is similar to that reported by
322 Amjadi, Nazari [20], who showed that NLPs fulfill a valuable role in the protection of the
323 film's crystalline nature according to XRD analysis.

324 **3.6.3. Antimicrobial activity**

325 The test for antimicrobial properties was based on the determination of the inhibition zone
326 diameter around the film discs containing the antimicrobial substance. The inhibition zone
327 values for *E. coli* O157:H7 and *S. aureus* were 1.6 and 2.23 mm, respectively. The larger the
328 diameter of the inhibition zone, the greater the desirability of the film antimicrobial properties.
329 The optimum film exerted a stronger effect against *S. aureus* (Gram-positive) than *E. coli*
330 (Gram-negative). This is due to the outer membrane structure of *E. coli*; Gram-negative
331 bacteria have a multiplex cell wall comprised of a peptidoglycan layer and an extra outer
332 membrane. Notably, the outer membrane of a Gram-negative strain reduces the effect of
333 betanin's phenolic groups and minimizes the permeability of radicals like reactive oxygen
334 species [35]. In this light, Wu, Liu [36] reported that the enhanced antibacterial activity of films
335 containing cinnamon essential oil NLPs probably is due to the protection of the compound
336 loaded within the NLPs against the environmental conditions and the subcellular size of the
337 NLPs, which increases their cellular absorption and leads to enhanced antimicrobial activity
338 and decreased mass transfer resistance. In agreement with our findings, Amjadi, Nazari [20]
339 noted that the antibacterial activity of NLP-containing film samples was higher against *S.*
340 *aureus* than *E. coli*.

341 **4. Conclusion**

342 In this study, betanin NLPs were introduced to the WPI/PG matrix to prepare a novel
343 bionanocomposite film with prominent mechanical and functional properties. The
344 incorporation of the NLPs led to decreased WVP and solubility together with enhanced
345 mechanical, antimicrobial, and antioxidant characteristics in the bionanocomposite films. The
346 films were opaque due to the presence of PG. Furthermore, the interaction of PG with betanin
347 WPI resulted in decreased solubility. However, the addition of PG caused a decrease in
348 mechanical strength. The optimum packaging film was obtained at 6.9% betanin NLPs and
349 1.5% PG. The results of the current research showed that bio-nanocomposites based on
350 WPI/PG/NLPs may have potential applications as a primary coating or packaging material for
351 fresh and/or perishable products. Investigating the PG and WPI interaction at different pHs as
352 well as the effect of the glycerol to PG/WPI ratio is recommended for further studies.

353

354

355 **Declarations**

356 **Funding:** Not applicable

357 **Conflicts of interest:** None

358 **Availability of data and material:** Not applicable

359 **Code availability:** Not applicable

360 **Authors' contributions:**

361 **Zahra Ghasempour:** Conceptualization; Project administration; Writing – original draft

362 **Sepideh khodaeivandi:** Investigation; Methodology; Validation; Writing - original draft

363 **Hossein Ahangari:** Investigation; Methodology; Writing - original draft

364 **Hamed Hamishehkar:** Resources; Supervision; Writing – review & editing

365 **Sajed Amjadi:** Investigation; Methodology; Writing – review & editing

366 **Ehsan Moghaddas Kia:** Conceptualization; Formal analysis; Writing - original draft

367 **Ali Ehsani:** Funding acquisition; Resources; Writing – review & editing

368

369

370 **References**

- 371 1. Salarbashi, D., et al., *Eco-friendly soluble soybean polysaccharide/nanoclay Na+*
372 *bionanocomposite: Properties and characterization*. Carbohydrate polymers, 2017.
373 **169**: p. 524-532. <https://doi.org/10.1016/j.carbpol.2017.04.011>
- 374 2. Castro-Rosas, J., et al., *Biopolymer films and the effects of added lipids, nanoparticles*
375 *and antimicrobials on their mechanical and barrier properties: a review*. International
376 Journal of Food Science & Technology, 2016. **51**(9): p. 1967-1978.
377 <https://doi.org/10.1111/ijfs.13183>
- 378 3. Farhan, A. and N.M. Hani, *Active edible films based on semi-refined κ-carrageenan:*
379 *Antioxidant and color properties and application in chicken breast packaging*. Food
380 Packaging and Shelf Life, 2020. **24**: p. 100476.
381 <https://doi.org/10.1016/j.fpsl.2020.100476>
- 382 4. Galus, S. and J. Kadzińska, *Whey protein edible films modified with almond and walnut*
383 *oils*. Food Hydrocolloids, 2016. **52**: p. 78-86.
384 <https://doi.org/10.1016/j.foodhyd.2015.06.013>
- 385 5. Khalesi, H., et al., *Effects of biopolymer ratio and heat treatment on the complex*
386 *formation between whey protein isolate and soluble fraction of Persian gum*. Journal
387 of Dispersion Science and Technology, 2017. **38**(9): p. 1234-1241.
388 <https://doi.org/10.1080/01932691.2016.1230064>
- 389 6. Emamverdian, P., et al., *Characterization and optimization of complex coacervation*
390 *between soluble fraction of Persian gum and gelatin*. Colloids and Surfaces A:
391 Physicochemical and Engineering Aspects, 2020. **607**: p. 125436.
392 <https://doi.org/10.1007/s10924-020-01906-5>
- 393 7. Abbasi, S., *Challenges towards characterization and applications of a novel*
394 *hydrocolloid: Persian gum*. Current Opinion in Colloid & Interface Science, 2017. **28**:
395 p. 37-45. <https://doi.org/10.1016/j.cocis.2017.03.001>
- 396 8. Pak, E.S., S.N. Ghaghelestani, and M.A. Najafi, *Preparation and characterization of a*
397 *new edible film based on Persian gum with glycerol plasticizer*. JOURNAL OF FOOD
398 SCIENCE AND TECHNOLOGY-MYSORE, 2020. [https://doi.org/10.1007/s13197-](https://doi.org/10.1007/s13197-020-04361-1)
399 [020-04361-1](https://doi.org/10.1007/s13197-020-04361-1)
- 400 9. Khezerlou, A., et al., *Development and characterization of a Persian gum–sodium*
401 *caseinate biocomposite film accompanied by Zingiber officinale extract*. Journal of
402 Applied Polymer Science, 2019. **136**(12): p. 47215. <https://doi.org/10.1002/app.47215>

- 403 10. Khodaei, D., K. Oltrogge, and Z. Hamidi-Esfahani, *Preparation and characterization*
404 *of blended edible films manufactured using gelatin, tragacanth gum and, Persian gum.*
405 LWT, 2020. **117**: p. 108617. <https://doi.org/10.1016/j.lwt.2019.108617>
- 406 11. Khorram, F., A. Ramezani, and S.M.H. Hosseini, *Shellac, gelatin and Persian gum*
407 *as alternative coating for orange fruit.* Scientia Horticulturae, 2017. **225**: p. 22-28.
408 <https://doi.org/10.1016/j.scienta.2017.06.045>
- 409 12. Moghaddas Kia, E., Z. Ghasempour, and M. Alizadeh, *Fabrication of an eco-friendly*
410 *antioxidant biocomposite: Zedo gum/sodium caseinate film by incorporating*
411 *microalgae (Spirulina platensis).* Journal of Applied Polymer Science, 2018. **135**(13):
412 p. 46024. <https://doi.org/10.1007/s10924-020-01906-5>
- 413 13. Golkar, A., A. Nasirpour, and J. Keramat, *β -lactoglobulin-Angum gum (Amygdalus*
414 *Scoparia Spach) complexes: Preparation and emulsion stabilization.* Journal of
415 Dispersion Science and Technology, 2015. **36**(5): p. 685-694.
416 <https://doi.org/10.1080/01932691.2014.919587>
- 417 14. Azarikia, F. and S. Abbasi, *Mechanism of soluble complex formation of milk proteins*
418 *with native gums (tragacanth and Persian gum).* Food Hydrocolloids, 2016. **59**: p. 35-
419 44. <https://doi.org/10.1016/j.foodhyd.2015.10.018>
- 420 15. Khan, M.I., *Plant betalains: Safety, antioxidant activity, clinical efficacy, and*
421 *bioavailability.* Comprehensive Reviews in Food Science and Food Safety, 2016.
422 **15**(2): p. 316-330. <https://doi.org/10.1111/1541-4337.12185>
- 423 16. Kia, E.M., Langroodi, A.M., Ghasempour, Z. and Ehsani, A., 2020. *Red beet extract*
424 *usage in gelatin/gellan based gummy candy formulation introducing Salix aegyptiaca*
425 *distillate as a flavouring agent.* Journal of Food Science and Technology, **57**(9),
426 pp.3355-3362. <https://doi.org/10.1007/s13197-020-04368-8>
- 427 17. Vieira Teixeira da Silva, D., et al., *Betanin, a natural food additive: Stability,*
428 *bioavailability, antioxidant and preservative ability assessments.* Molecules, 2019.
429 **24**(3): p. 458. <https://doi.org/10.3390/molecules24030458>
- 430 18. Ghasempour, Z., Javanmard, N., Langroodi, A.M., Alizadeh-Sani, M., Ehsani, A. and
431 Kia, E.M., 2020. *Development of probiotic yogurt containing red beet extract and basil*
432 *seed gum; techno-functional, microbial and sensorial characterization.* Biocatalysis
433 and Agricultural Biotechnology, **29**, p.101785.
434 <https://doi.org/10.1016/j.bcab.2020.101785>

- 435 19. Amjadi, S., et al., *Improvement in the stability of betanin by liposomal nanocarriers:*
436 *Its application in gummy candy as a food model.* Food chemistry, 2018. **256**: p. 156-
437 162. <https://doi.org/10.1016/j.foodchem.2018.02.114>
- 438 20. Amjadi, S., et al., *Multifunctional betanin nanoliposomes-incorporated*
439 *gelatin/chitosan nanofiber/ZnO nanoparticles nanocomposite film for fresh beef*
440 *preservation.* Meat Science, 2020: p. 108161.
441 <https://doi.org/10.1016/j.meatsci.2020.108161>
- 442 21. Peng, Y., Y. Wu, and Y. Li, *Development of tea extracts and chitosan composite films*
443 *for active packaging materials.* International Journal of Biological Macromolecules,
444 2013. **59**: p. 282-289. <https://doi.org/10.1016/j.ijbiomac.2013.04.019>
- 445 22. Jahed, E., et al., *Physicochemical properties of Carum copticum essential oil loaded*
446 *chitosan films containing organic nanoreinforcements.* Carbohydrate polymers, 2017.
447 **164**: p. 325-338. <https://doi.org/10.1016/j.carbpol.2017.02.022>
- 448 23. Alizadeh-Sani, M., et al., *Preparation of Active Nanocomposite Film Consisting of*
449 *Sodium Caseinate, ZnO Nanoparticles and Rosemary Essential Oil for Food Packaging*
450 *Applications.* Journal of Polymers and the Environment, 2020: p. 1-11.
451 <https://doi.org/10.1007/s10924-020-01906-5>
- 452 24. Aziz, S.G.-G. and H. Almasi, *Physical characteristics, release properties, and*
453 *antioxidant and antimicrobial activities of whey protein isolate films incorporated with*
454 *thyme (Thymus vulgaris L.) extract-loaded nanoliposomes.* Food and Bioprocess
455 Technology, 2018. **11**(8): p. 1552-1565.
456 <https://doi.org/10.1016/j.foodhyd.2019.105338>
- 457 25. Li, X., et al., *Gelatin films incorporated with thymol nanoemulsions: Physical*
458 *properties and antimicrobial activities.* International Journal of Biological
459 Macromolecules, 2020. **150**: p. 161-168.
460 <https://doi.org/10.1016/j.ijbiomac.2020.02.066>
- 461 26. Calva-Estrada, S.J., M. Jiménez-Fernández, and E. Lugo-Cervantes, *Protein-based*
462 *films: Advances in the development of biomaterials applicable to food packaging.* Food
463 Engineering Reviews, 2019. **11**(2): p. 78-92. [https://doi.org/10.1007/s12393-019-](https://doi.org/10.1007/s12393-019-09189-w)
464 [09189-w](https://doi.org/10.1007/s12393-019-09189-w)
- 465 27. Zhang, X., et al., *High performance PVA/lignin nanocomposite films with excellent*
466 *water vapor barrier and UV-shielding properties.* International journal of biological
467 macromolecules, 2020. **142**: p. 551-558.
468 <https://doi.org/10.1016/j.ijbiomac.2019.09.129>

- 469 28. Cejudo-Bastante, M.J., et al., *Optical, structural, mechanical and thermal*
470 *characterization of antioxidant ethylene vinyl alcohol copolymer films containing*
471 *betalain-rich beetroot*. Food Packaging and Shelf Life, 2020. **24**: p. 100502.
472 <https://doi.org/10.1016/j.fpsl.2020.100502>
- 473 29. Marín-Peñalver, D., et al., *Carboxymethyl cellulose films containing nanoliposomes*
474 *loaded with an angiotensin-converting enzyme inhibitory collagen hydrolysate*. Food
475 hydrocolloids, 2019. **94**: p. 553-560. <https://doi.org/10.1016/j.foodhyd.2019.04.009>
- 476 30. Doost, A.S., et al., *Pickering stabilization of thymol through green emulsification using*
477 *soluble fraction of almond gum–Whey protein isolate nano-complexes*. Food
478 hydrocolloids, 2019. **88**: p. 218-227. <https://doi.org/10.1016/j.foodhyd.2018.10.009>
- 479 31. Alizadeh-Sani, M., A. Khezerlou, and A. Ehsani, *Fabrication and characterization of*
480 *the bionanocomposite film based on whey protein biopolymer loaded with TiO₂*
481 *nanoparticles, cellulose nanofibers and rosemary essential oil*. Industrial crops and
482 products, 2018. **124**: p. 300-315. <https://doi.org/10.1016/j.indcrop.2018.08.001>
- 483 32. Petera, B., et al., *Characterization of arabinogalactan-rich mucilage from Cereus*
484 *triangularis cladodes*. Carbohydrate Polymers, 2015. **127**: p. 372-380.
485 <https://doi.org/10.1016/j.carbpol.2015.04.001>
- 486 33. Ghadetaj, A., H. Almasi, and L. Mehryar, *Development and characterization of whey*
487 *protein isolate active films containing nanoemulsions of Grammosciadium ptrocarpum*
488 *Bioss. essential oil*. Food packaging and shelf life, 2018. **16**: p. 31-40.
489 <https://doi.org/10.1016/j.fpsl.2018.01.012>
- 490 34. Acquah, C., et al., *Formation and characterization of protein-based films from yellow*
491 *pea (Pisum sativum) protein isolate and concentrate for edible applications*. Current
492 Research in Food Science, 2020. **2**: p. 61-69. <https://doi.org/10.1016/j.crfs.2019.11.008>
- 493 35. Shankar, S., et al., *Preparation, characterization, and antimicrobial activity of*
494 *gelatin/ZnO nanocomposite films*. Food Hydrocolloids, 2015. **45**: p. 264-271.
495 <https://doi.org/10.1016/j.foodhyd.2014.12.001>
- 496 36. Wu, J., et al., *The preparation, characterization, antimicrobial stability and in vitro*
497 *release evaluation of fish gelatin films incorporated with cinnamon essential oil*
498 *nanoliposomes*. Food Hydrocolloids, 2015. **43**: p. 427-435.
499 <https://doi.org/10.1016/j.foodhyd.2014.06.017>

500

501 **Table 1.** Regression coefficients of the second-order polynomial model for the response
 502 variables.

Response	Regression equation	Brief model
Solubility	$\text{Solubility} = 1.68 - 0.08 \times A^a - 0.14 \times B^b + 0.05 \times AB - 0.08 \times A^2$	R-sq = 0.92 R-sq(adj) = 0.88
Thickness	$\text{Thickness} = 0.24 + 0.01 \times A + 0.02 \times B - 0.01 \times AB$	R-sq = 0.96 R-sq(adj) = 0.95
AC ^c	$\text{Antioxidant activity} = 54.5 + 19.47 \times A + 2.98 \times B - 3.94 \times A^2 + 2.01 \times B^2$	R-sq = 0.99 R-sq(adj) = 0.99
WVP ^d	$\text{WVP} = 5.99\text{E-}07 + 2.14\text{E-}09 \times A + 2.03\text{E-}08 \times B - 6.28\text{E-}08 \times AB + 6.26\text{E-}08 \times A^2$	R-sq = 0.89 R-sq(adj) = 0.82
UTS ^e	$\text{UTS} = 4.79 + 0.32 \times A - 0.31 \times B - 0.78 \times A^2$	R-sq = 0.89 R-sq(adj) = 0.88
EB ^f	$\text{EB} = 99.4 - 2570.73A - 1.11B + 33.21A \times B + 104852.35A^2 + 0.18B^2$	R-sq = 0.99 R-sq(adj) = 0.98
YM ^g	$\text{YM} = 77.52 + 3.03 \times A - 9.4 \times B - 22.23 \times A^2$	R-sq = 0.80 R-sq(adj) = 0.74

503 ^a Betanin nanoliposomes % (W/V), ^b Persian gum % (W/V), ^c antioxidant capacity, ^d water vapor
 504 permeability, ^e ultimate tensile strength, ^f elongation at break, ^g Young's modulus

505 **Table 2.** Parameters response of optimal film using response surface methodology (RSM)

NLP^a (%)	PG^b (%)	WVP^c (g/Pa.s.m)	Solubility (%)	AC^d (%)	UTS^e (Mpa)	YM^f (Mpa)	L^g	a^h	bⁱ	Desirability
6.90%	1.5%	5.46	1.57%	63.45%	4.64	70.75	56.74	-5	29.88	0.71

506 ^a Nanoliposomes, ^b Persian gum, ^c water vapor permeability, ^d antioxidant capacity, ^e ultimate tensile
507 strength, ^f Young's modulus, ^g lightness, ^h red/green, ⁱ yellow/blue
508

509 **Figure captions:**

510 **Schematic 1.** Chemical structure of betanin

511 **Figure 1.** The interaction effect of betanin nanoliposomes and Persian gum amount on the water
512 vapor permeability in the whey protein isolate-based edible film (toward red indicating higher
513 values of response and toward blue indicating lower values of response).

514 **Figure 2.** The effect of betanin nanoliposomes and Persian gum (minimum [0%] and maximum
515 level [2%]) on the antioxidant capacity of the whey protein isolate-based edible film.

516 **Figure 3.** The betanin nanoliposomes and Persian gum effect on (A) ultimate tensile strength and
517 (B) Young's modulus of the whey protein isolate-based edible film (toward red indicating higher
518 values of response and toward blue indicating lower values of response).

519 **Figure 4.** SEM images: (A) control sample; (B) optimal film containing 6.9% betanin
520 nanoliposomes and 1.5% Persian gum.

521 **Figure 5.** XRD spectra: (A) pure whey protein isolate; (B) pure Persian gum; (C) betanin
522 nanoliposomes; (D) optimal film sample (6.9% betanin nanoliposomes and 1.5% Persian gum).

Figures

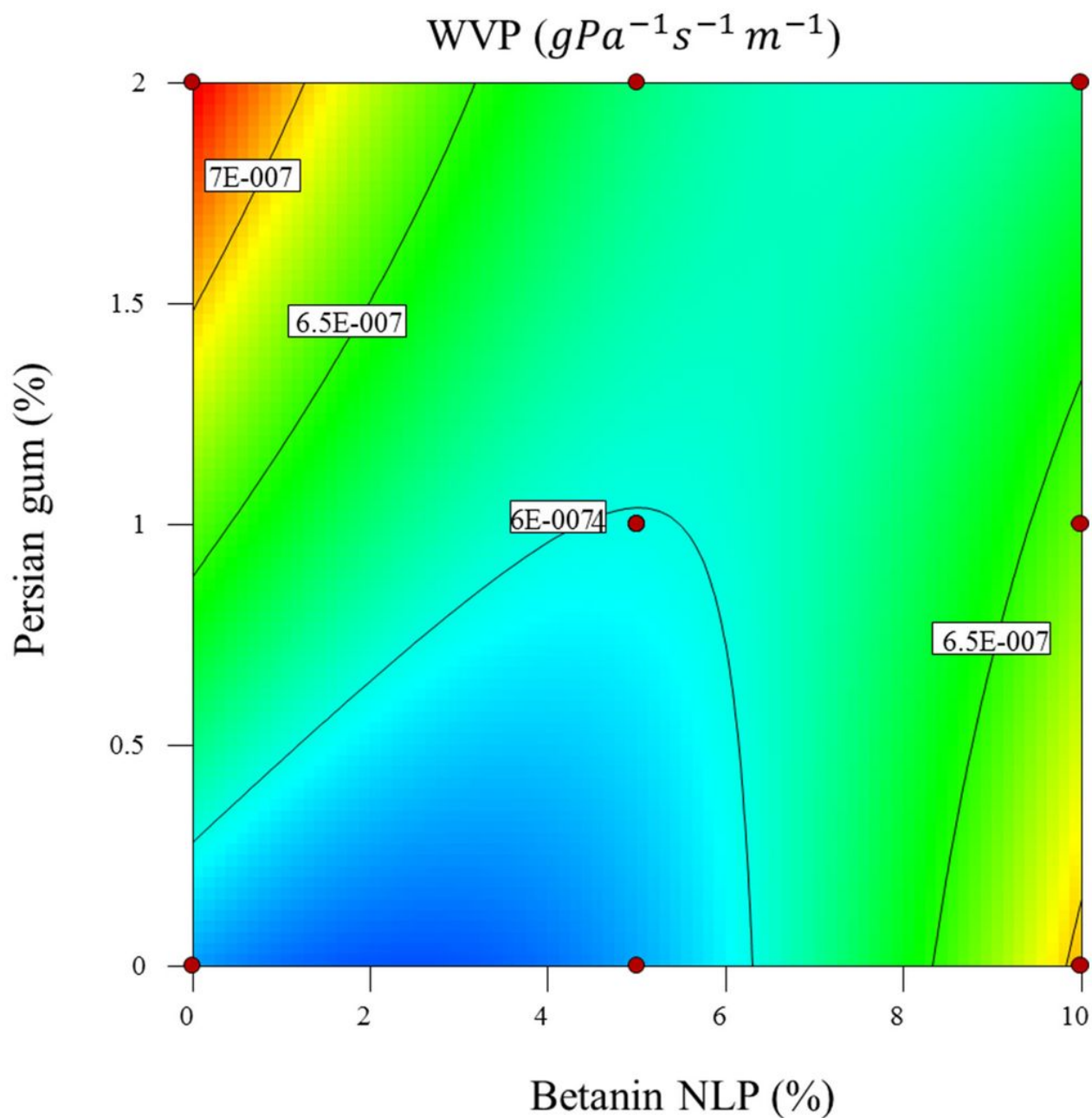


Figure 1

The interaction effect of betanin nanoliposomes and Persian gum amount on the water vapor permeability in the whey protein isolate-based edible film (toward red indicating higher values of response and toward blue indicating lower values of response).

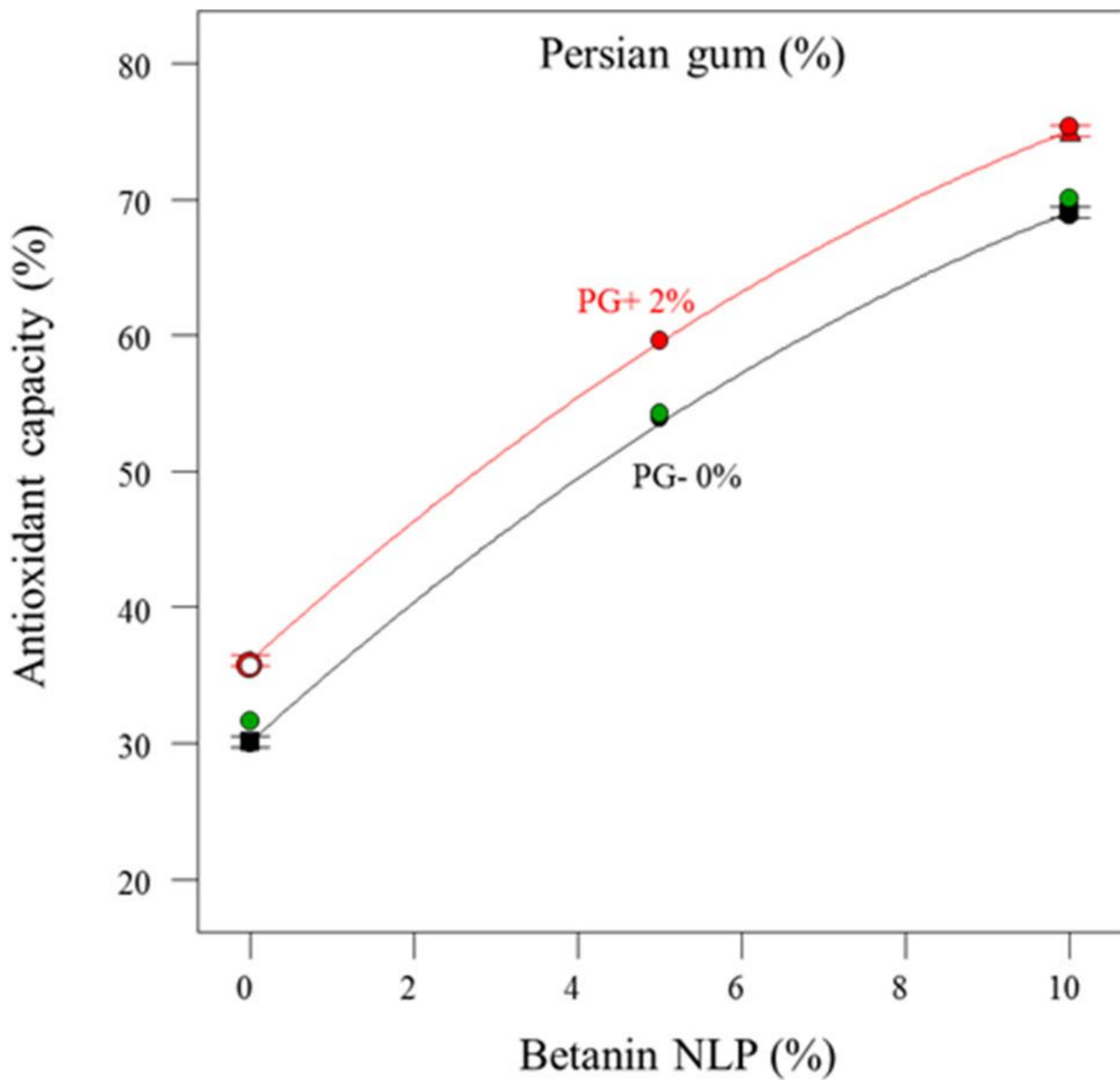


Figure 2

The effect of betanin nanoliposomes and Persian gum (minimum [0%] and maximum level [2%]) on the antioxidant capacity of the whey protein isolate-based edible film.

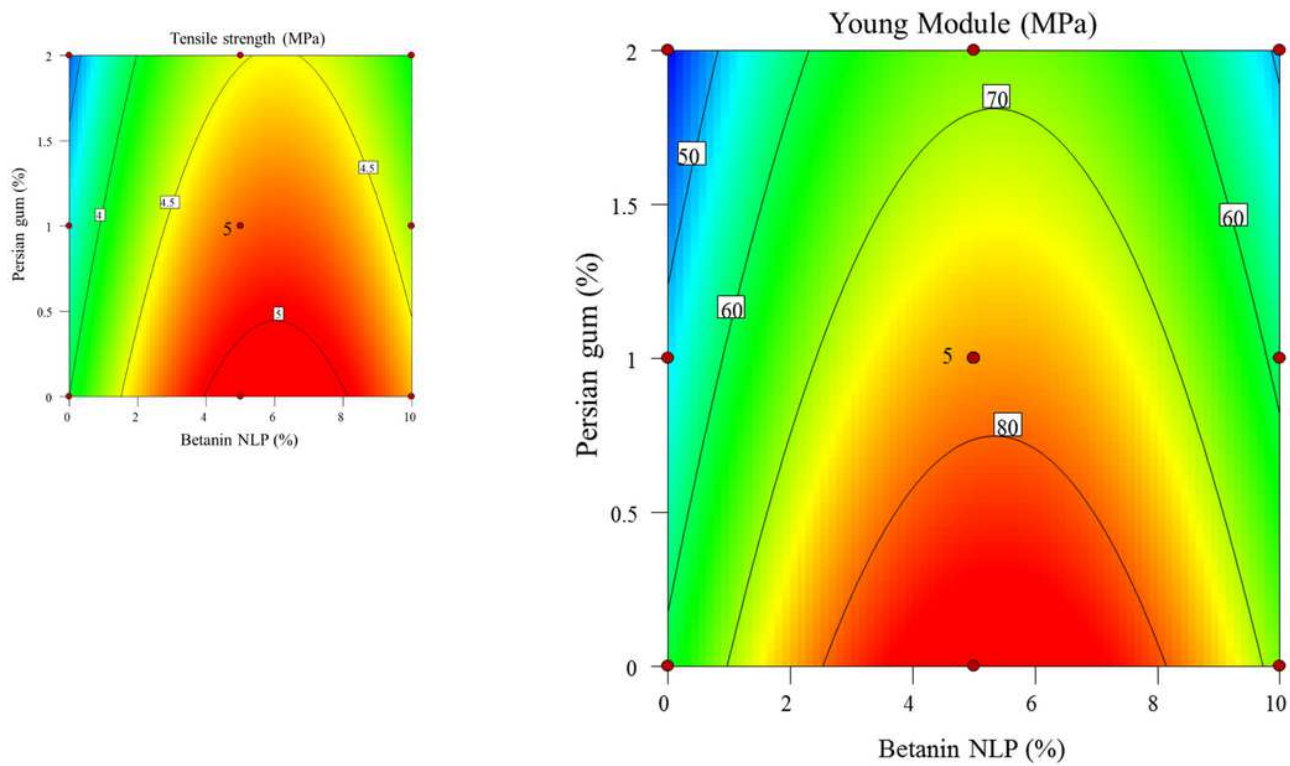


Figure 3

The betanin nanoliposomes and Persian gum effect on (A) ultimate tensile strength and (B) Young's modulus of the whey protein isolate-based edible film (toward red indicating higher values of response and toward blue indicating lower values of response).

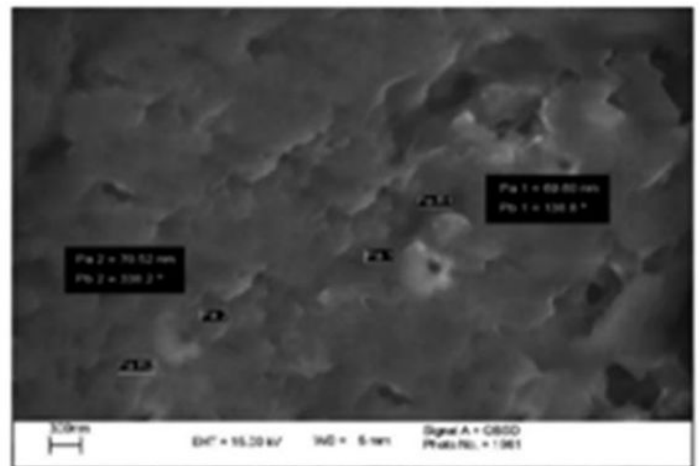
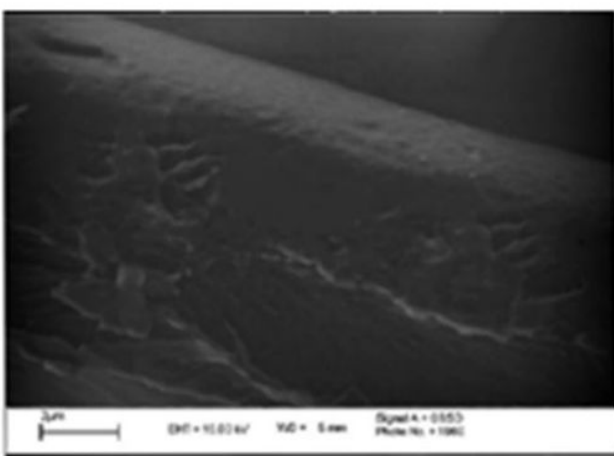


Figure 4

SEM images: (A) control sample; (B) optimal film containing 6.9% betanin nanoliposomes and 1.5% Persian gum.

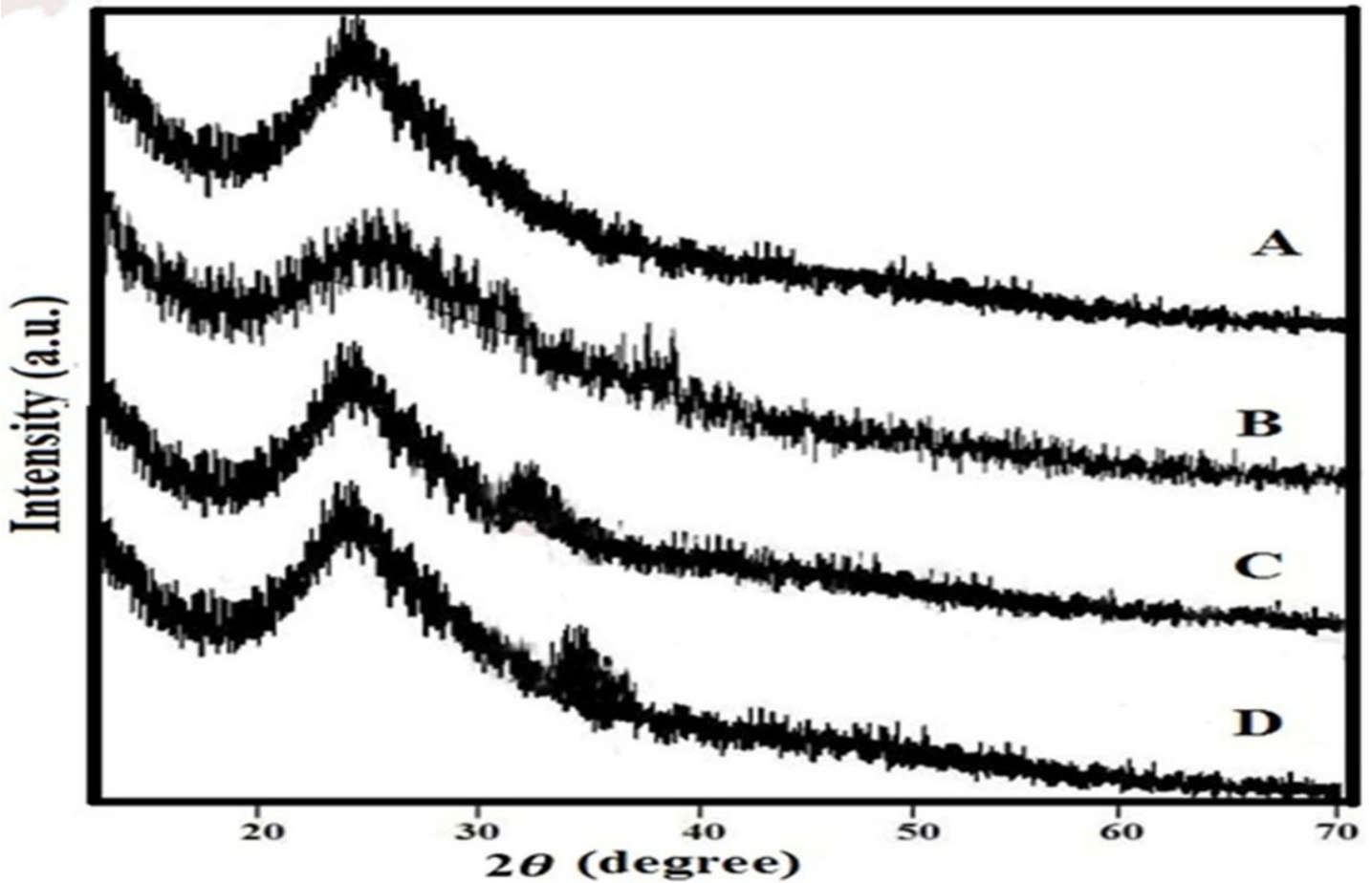


Figure 5

XRD spectra: (A) pure whey protein isolate; (B) pure Persian gum; (C) betanin nanoliposomes; (D) optimal film sample (6.9% betanin nanoliposomes and 1.5% Persian gum).

Image not available with this version

Figure 6

Schematic 1. Chemical structure of betanin